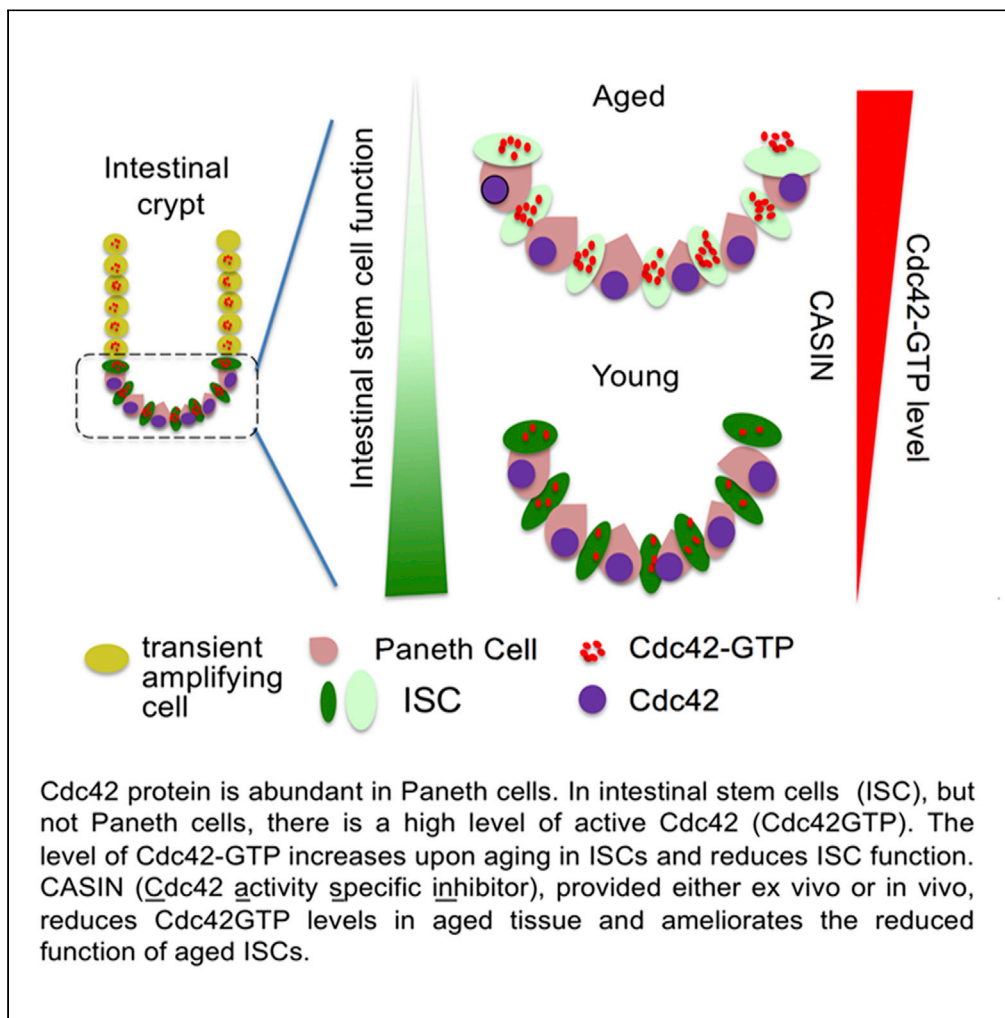


Article

Suppression of elevated Cdc42 activity promotes the regenerative potential of aged intestinal stem cells



Kodandaramireddy Nalapareddy, Aishlin Hassan, Leesa L. Sampson, Yi Zheng, Hartmut Geiger

hartmut.geiger@uni-ulm.de

Highlights

Intestinal stem cells show high RhoGTPase Cdc42 activity compared to Paneth cells

Cdc42 activity is further increased in aged intestinal stem cells (ISCs)

Attenuation of Cdc42 activity ex vivo or in vivo improves the function of aged ISCs



Article

Suppression of elevated Cdc42 activity promotes the regenerative potential of aged intestinal stem cells

Kodandamireddy Nalapareddy,¹ Aishlin Hassan,¹ Leesa L. Sampson,¹ Yi Zheng,¹ and Hartmut Geiger^{1,2,*}

SUMMARY

Homeostasis in the intestinal epithelium is maintained by Lgr5-positive intestinal stem cells (ISCs) located at the base of the crypt. The function of ISCs is reduced upon aging which leads to a decline of regeneration of the intestinal epithelium. We report that aged intestinal crypts present with an elevated activity of the small RhoGTPase Cdc42. Elevation of Cdc42 activity in young animals by genetic means causes premature ISC aging, whereas pharmacological suppression of elevated Cdc42 activity restores organoid formation potential *in vitro*. Consistent with a critical role of elevated Cdc42 activity in aged ISCs for a reduced regenerative capacity of aged ISCs, suppression of Cdc42 activity *in vivo* improves crypt regeneration in aged mice. Thus, pharmacological reduction of Cdc42 activity can improve the regeneration of aged intestinal epithelium.

INTRODUCTION

The regenerative capacity of intestine decreases upon aging. Organ homeostasis in the intestine is maintained by intestinal stem cells (ISCs) (Geiger et al., 2013; Nalapareddy et al., 2017; Rando, 2006; Rossi et al., 2008). A decline in ISC function is a main reason for the impaired regeneration of intestinal epithelium upon aging (Nalapareddy et al., 2017). ISCs express the marker gene Lgr5 and are located next to differentiated Paneth cells at the base of the intestinal crypt (Barker et al., 2007). To function properly under homeostasis, ISCs differentiate into highly proliferative transient amplifying (TA) cells. Upon their migration from the crypt base to the villus, TA cells further differentiate into mature cell types including cells in the intestinal villus made of enterocytes, goblet cells, and enteroendocrine cells (Barker et al., 2008).

The small RhoGTPase Cdc42 cycles between an active, GTP-bound form (Cdc42-GTP) and an inactive, GDP-bound form (Florian et al., 2012; Wang et al., 2007). It is thought that biological activity of Cdc42 is regulated by its active form, i.e., the level of Cdc42-GTP. The relative ratio of active Cdc42 is elevated in various tissues of aged mice compared to that of young mice, whereas animals in which Cdc42 activity is increased by genetic means show diverse premature aging phenotypes (Wang et al., 2006, 2007). It is possible that there is a causative link between Cdc42 activity and aging, and increased Cdc42 activity has indeed been reported to be a causative stem cell intrinsic mechanism for the aging of hematopoietic stem cells (HSCs) (Florian et al., 2012). For ISCs, their regeneration capacity declines upon aging (Nalapareddy et al., 2017), and multiple mechanisms including changes in Wnt signaling could be involved in the process. We show here that an aging-associated increase in the Cdc42 activity in ISCs causes a decline in ISC function and impairs intestinal epithelial regeneration. Suppression of Cdc42 activity can ameliorate ISC regeneration *in vitro*, and pharmacologic targeting of Cdc42 critically enhances intestinal regeneration upon stress *in vivo* upon aging. Our studies imply that a tight regulation of the Cdc42 activity is critical for maintaining tissue homeostasis within the intestine during aging and that suppression of aging-related increased Cdc42 activity allows for enhanced tissue regeneration *in vivo*.

RESULTS

Cdc42 activity is increased in aged intestinal crypts

We started by investigating the level of Cdc42 activity in aged intestinal crypts. Immunofluorescence (IF) staining on the intestinal epithelium identified a high level of active Cdc42 (Cdc42GTP) in ISCs (Lgr5GFP + cells) (Figures 1A and S1A) but less so in the differentiated Paneth cells (lysozyme-positive cells) that surround ISCs (Figure 1B, Videos S1 and S2). Analysis of Cdc42GTP levels in isolated ISCs and Paneth cells

¹Division of Experimental Hematology and Cancer Biology, Cincinnati Children's Hospital Medical Center and University of Cincinnati, 3333 Burnet Avenue, Cincinnati, OH 45229, USA

²Lead contact

*Correspondence:

hartmut.geiger@uni-ulm.de
<https://doi.org/10.1016/j.isci.2021.102362>



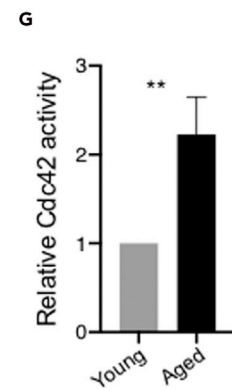
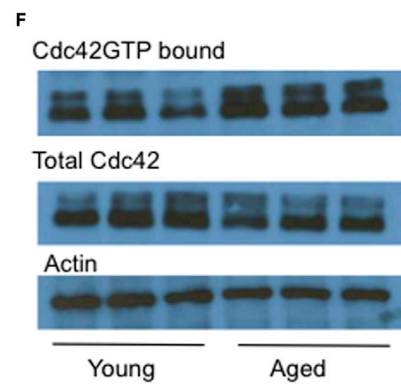
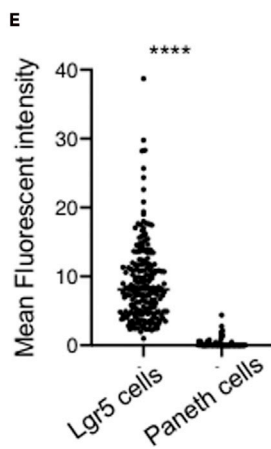
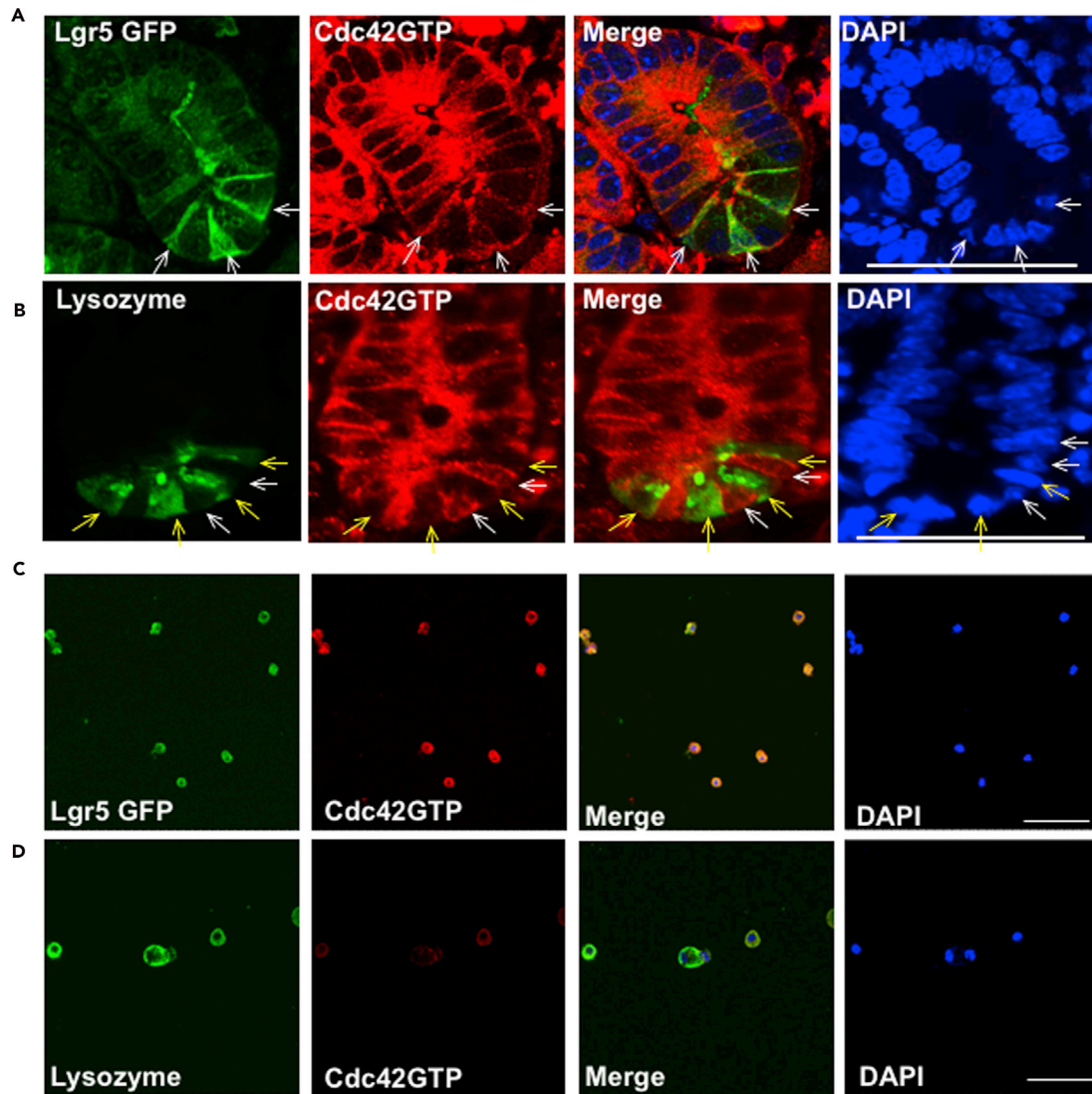


Figure 1. Cdc42 activity is increased in aged intestinal crypts

(A) Immunofluorescence staining of Cdc42 GTP (red), Lgr5 eGFP (green, white arrows), and DAPI (blue) in aged murine intestinal crypts (representative pictures, scale bar, 50 μ m)
(B) Immunofluorescence staining of Cdc42 GTP (red, white arrows), lysozyme (green, yellow arrows), and DAPI (blue) in aged murine intestinal crypts (representative pictures, scale bar, 50 μ m)
(C) Immunofluorescence staining of Cdc42 GTP (red), Lgr5 GFP (green), and DAPI (blue) in murine sorted Lgr5 GFP sorted cells (representative pictures, scale bar, 50 μ m)
(D) Immunofluorescence staining of Cdc42 GTP (red), lysozyme (green), and DAPI (blue) in murine sorted CD24-positive Paneth cells (representative pictures), scale bar, 50 μ m.
(E) Dot plot showing Cdc42GTP mean fluorescent intensity in the indicated cell types. (Bar in graph indicates median)
(F) Western blot of Cdc42 pull-down experiment to quantify the relative amount of Cdc42 GTP, Cdc42, and β -actin protein in young and aged crypts.
(G) Relative level of Cdc42 GTP normalized to total Cdc42 and β -actin (n = 5 per group) in aged compared to young crypts. (A to G): n = 3 to 5 mice/ experimental group. *p < 0.05, **p < 0.01, ***p < 0.001. Error bars represent standard deviation (SD).

by IF revealed that the level of Cdc42GTP was elevated in ISCs compared to Paneth cells (Figures 1C–1E and S1B–S1D). In contrast, total Cdc42 (both GDP and GTP bound) was primarily detected in differentiated cells like Paneth cells (here MMP7-positive cells) in the crypt but less in ISCs or TA cells in both young and aged intestines (Figures S1E and S1F). The relative Cdc42 activity (GTP bound over total Cdc42) is thus in general higher in compartments like ISCs and TA cells compared to, for example, Paneth cells. Next, we tested whether there is a difference in the relative Cdc42 activity between young and aged crypts via the more sensitive effector pull-down assay. Aged intestinal crypts showed an ~2-fold increase in Cdc42 activity compared to that of young crypts (Figures 1F and 1G). An elevated activity of Cdc42 might therefore limit ISC-driven regeneration up on aging.

An aging-associated increase in Cdc42 activity in aged HSCs has been shown to be responsible for an increase in the frequency of HSCs with an apolar distribution of the epigenetic marker H4K16Ac, while young HSCs primarily present with a polar distribution. A higher frequency of cells with an apolar distribution of H4K16ac is a novel hallmark of aged HSCs (Florian et al., 2012, 2018). A reduced frequency of cells with a polar distribution of H4K16Ac was also observed in ISCs *in vivo* upon aging (Figures S2A–S2C, Videos S3 and S4), which implies that a reduced frequency of the polar distribution of H4K16ac might be a shared novel marker of aged stem cells.

Genetically elevated levels of Cdc42 in young mice confers aging-associated phenotypes on the intestine

If the increase in Cdc42 activity upon aging in the intestinal crypts was a causative factor for age-related phenotypes, then increasing Cdc42 activity in young mice should recapitulate aging phenotypes in already young animals. To determine the extent to which elevated Cdc42 activity in young animals causes aging-related phenotypes in the intestine, we analyzed genetically modified mice (Cdc42GAP^{-/-} animals) that present with constitutively elevated Cdc42 activity in almost all tissue analyzed so far (Wang et al., 2006, 2007) including crypts (S3A and S3B). Cdc42GAP is a negative regulator of Cdc42 which catalyzes GTP hydrolysis to inactivate Cdc42. Genetic deletion of Cdc42GAP causes a constitutively elevated Cdc42 activity compared to that in control animals (Wang et al., 2007). Analysis of hallmarks of intestinal aging (Nalapareddy et al., 2017) revealed an increase in crypt depth and increase in villus length in young Cdc42GAP^{-/-} animals compared to wild-type controls (Figures 2A, 2B, and S3C), while the number of Paneth cells was reduced (Figures S3D and S3E). Quantification of phospho-histone 3 (pH3) staining demonstrated a reduction in proliferative and thus pH3-positive cells in crypts in Cdc42GAP^{-/-} mice (Figures 2C and 2D). *In situ* hybridization for the ISC marker Olfm4 indicated presence of Olfm4 cells and thus ISCs in crypts of Cdc42GAP^{-/-} and controls mice (Figure 2E). To further analyze ISCs, we generated Cdc42GAP^{-/-}, Lgr5-eGFP-IRES-CreERT2 mice (data not shown). Surprisingly, the GFP expression linked to Lgr5 expression was muted in Cdc42GAP^{-/-}, Lgr5-eGFP-IRES-CreERT2 mice. It is known that the GFP expression in crypts of the Lgr5 GFP mouse can be quite mosaic (Barker et al., 2007), but it remains unclear why it is actually absent in Cdc42GAP^{-/-} animals. However, RNA-FISH (fluorescent *in situ* hybridization) analyses for expression of Lgr5 in crypts of Cdc42GAP^{-/-} mice confirmed a similar frequency of Lgr5-positive ISCs in Cdc42GAP^{-/-} mice and their littermate controls (Figures 2F and 2G), indicating that the decline in proliferation in the Cdc42GAP^{-/-} intestinal crypts is not simply a consequence of a reduced number of ISCs in Cdc42GAP^{-/-} animals. Quantitative gene expression analyses by real-time reverse transcription - polymerase chain reaction on a large number of established marker genes indicative of ISC identity and/or function such as *Ascl2*, *Olfm4*, β -catenin, *Lrig1*, *Hopx1*, *Sox9*, and *CcnD1* showed reduced expression in the crypts of Cdc42GAP^{-/-}

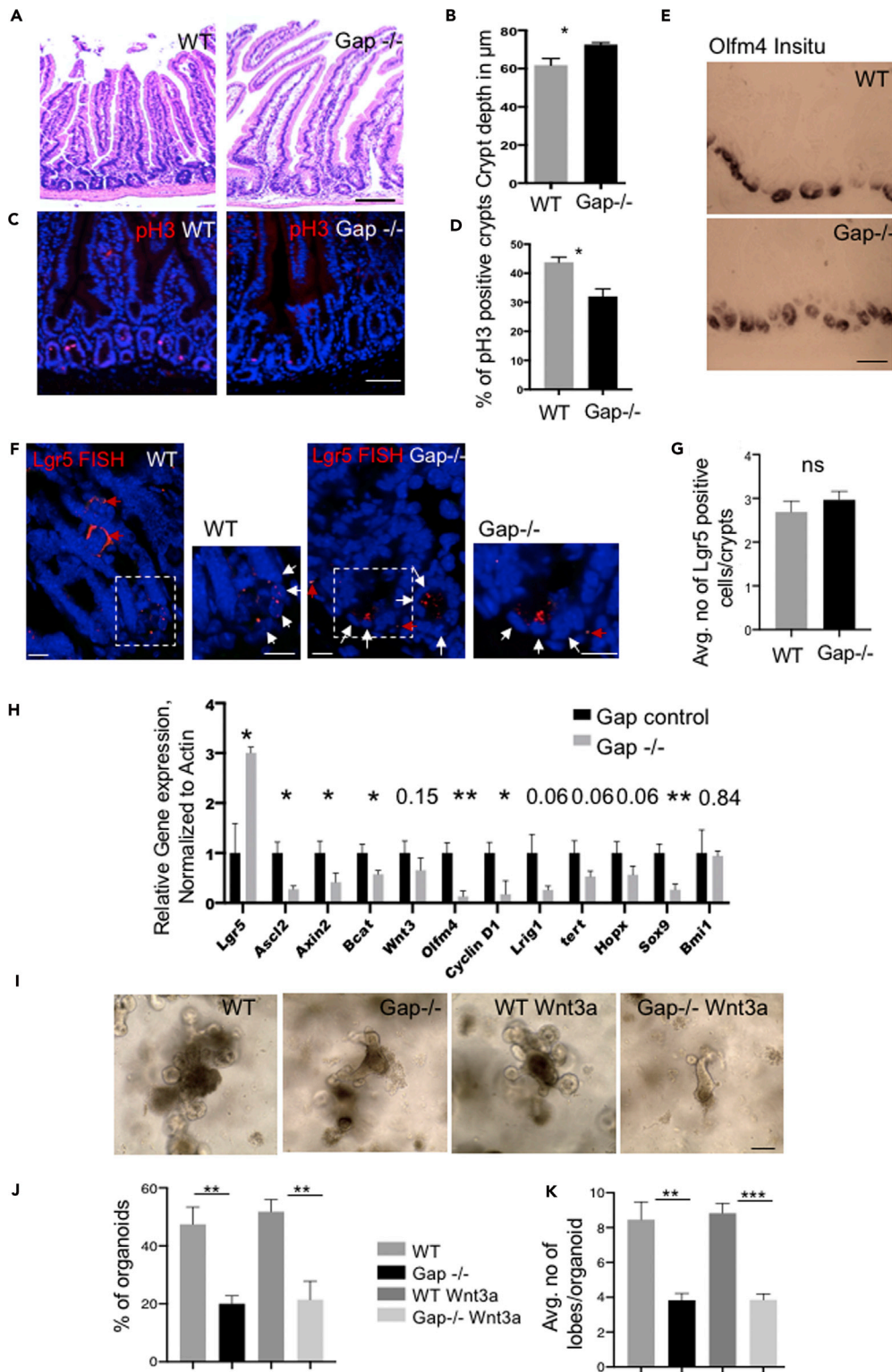


Figure 2. Genetically elevated levels of Cdc42 in young mice confer aging-associated phenotypes on the intestine

(A) Representative picture of IHC staining in wild-type (WT) littermate control and Cdc42GAP knockout mouse (Gap) intestine, measuring crypt size. Scale bar, 100 μ m.

(B) Histogram showing crypt depth in the proximal part of mice in the indicated genotypes.

Figure 2. Continued

- (C) Representative pictures of phospho-histone 3 (pH3) staining in WT and Gap mouse intestinal crypts. Scale bar, 50 μm .
- (D) Number of pH3-positive cells per crypt in WT and Gap intestine.
- (E) Representative picture of *Olfm4* *in situ* hybridization on WT and Gap mouse intestine. Scale bar, 100 μm . A blue/purple color indicates *Olfm4* *in situ* staining.
- (F) Representative picture of *Lgr5* FISH in WT and *Cdc42GAP* knockout mouse intestinal crypts. Scale bar, 10 μm . (White arrows indicate *Lgr5*-positive staining; red arrows indicate background staining).
- (G) Histogram showing average number of *Lgr5*-positive cells per crypt.
- (H) *Lgr5*, *Ascl2*, *Axin2*, β *catenin*, *Wnt3*, *Olfm4*, *Cyclin D1*, *Lrig1*, *Tert*, *HopX1*, *Sox 9*, and *Bmi1* expression normalized to β *actin* transcript levels in young and aged crypts of mouse small intestine.
- (I) Representative picture of organoids of WT and Gap intestinal crypts and WT and Gap intestinal crypts with *Wnt3a* treatment after one passage. Scale bar, 100 μm .
- (J) Percentage of organoid growth after one passage in the indicated genotypes/treatments.
- (K) Number of lobes per organoid in organoids derived from WT and Gap crypts (with and without *Wnt3a* treatment) of mouse small intestine after 1 week. (A to H) $n = 3$ to 5 mice per experimental group. * $p < 0.05$, ** $p < 0.01$, *** $p < 0.001$. Error bars represent standard deviation (SD).

mice compared to controls (Figure 2H). While it has been reported that the expression of *Lgr5* is regulated by *Ascl2* (van der Flier et al., 2009), the change in level of expression of *Lgr5* was high (Figure 2H) and was interestingly not linked to the change in the (reduced) level of expression of *Ascl2* (Figure 2H) in *Cdc42GAP*^{-/-} crypts.

The organoid formation assay is a widely used *in vitro* system to determine ISC function (Barker et al., 2007; Nalapareddy et al., 2017). Crypts from aged intestine show a decline in organoid formation capability (Nalapareddy et al., 2017). We further observed a severe decline in organoid formation of crypts from *Cdc42GAP*^{-/-} mice compared to that of crypts from control animals (Figures 2I–2K). The level of expression of key components of the canonical Wnt signaling cascade, e.g. *Ascl2* and β -catenin, was reduced in crypts of *Cdc42GAP*^{-/-} mice. We recently demonstrated that reduced canonical Wnt signaling in aged crypts is one mechanism resulting in the decline of organoid formation of aged crypts (Nalapareddy et al., 2017) and that activation of canonical Wnt signaling by the addition of the canonical Wnt ligand *Wnt3a* could rescue reduced organoid formation of aged intestinal crypts (Nalapareddy et al., 2017). As Paneth cells are one of the main sources of Wnts for ISCs (Pentimikko et al., 2019; Sato et al., 2011), the impaired ability of *Cdc42GAP*^{-/-} crypts to form organoids might be linked to the reduced Paneth cell number in these crypts (Figures S3D and S3E). If true, addition of exogenous Wnts to the organoid culture might then rescue the organoid formation ability of *Cdc42GAP*^{-/-} crypts. However, addition of *Wnt3a* to organoids derived from *Cdc42GAP*^{-/-} crypts failed to rescue the reduced organoid formation of *Cdc42GAP*^{-/-} crypts (Figures 2I–2K). Genetically elevated *Cdc42* activity is thus likely dominant over changes in canonical Wnt signaling in *Cdc42GAP*^{-/-} mouse intestinal crypts. However, we cannot exclude that additional (not yet known) functions of Paneth cells apart from Wnt secretion might play an additional role in regulating ISC function.

Suppression of elevated *Cdc42* activity enhances the function of aged ISCs

Analysis of *Cdc42GAP*^{-/-} mouse intestinal crypts support that elevated *Cdc42* activity upon aging is possibly causative for the decline of organoid formation of aged crypts and ISC function. Suppression of *Cdc42* activity in aged crypts might consequently attenuate the decline in the organoid-forming activity of aged crypts. Transient inhibition (overnight) of the elevated activity of *Cdc42* in aged crypts with a specific small molecule compound CASIN (*Cdc42* activity-specific inhibitor) (Florian et al., 2012; Florian et al., 2018; Liu et al., 2019) at 0.5 μM restored the organoid formation frequency of aged intestinal crypts as well as the number of lobes per organoid, almost to the level seen in the organoids from young animals (Figures 3A–3C and S3F–S3H). Most strikingly, CASIN treatment enhanced the organoid formation ability of isolated aged *Lgr5* eGFP^{hi} ISCs compared to the vehicle-treated aged *Lgr5* eGFP^{hi} ISCs (Figures 3D and 3E), indicating that elevated *Cdc42* activity within ISCs is an underlying mechanism in the aging-related reduced function of ISC.

Modulation of *Cdc42* activity *in vivo* enhances the regeneration of aged crypts upon stress

As the function of aged ISCs was enhanced by *in vitro* inhibition of *Cdc42* activity, we next thought to investigate if *in vivo* suppression of *Cdc42* activity might improve ISC-driven regeneration of the aged intestinal epithelium. CASIN treatment of animals by i.p. (50mg/kg) once a day for two consecutive days reduced the level of *Cdc42*-GTP activity in intestinal crypts of aged animals to that of young crypts (Figures 4A–4C). To analyze crypt regeneration upon this modulation of *Cdc42* activity in aged crypts, we employed a recently

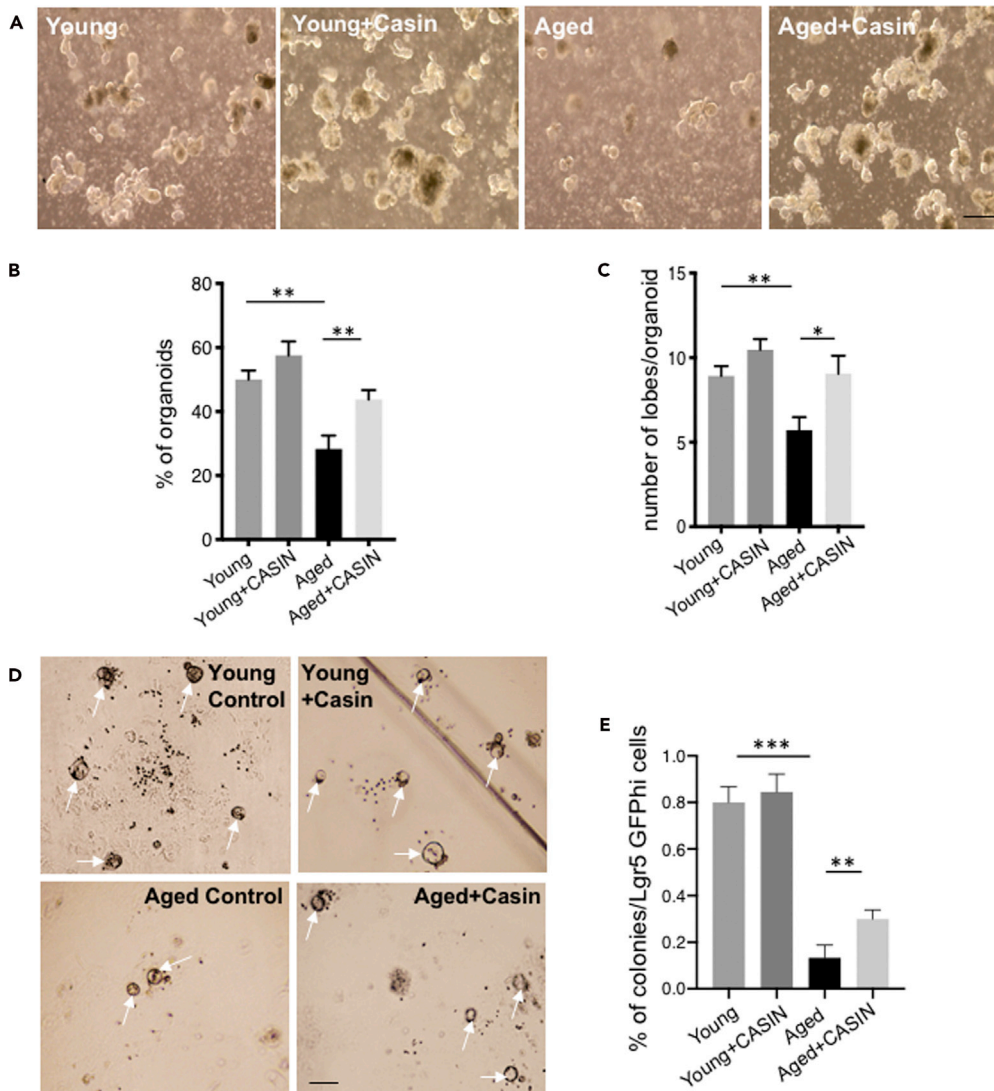


Figure 3. Suppression of elevated Cdc42 activity ameliorates regeneration of organoids

(A) Organoids formed from young and aged intestinal crypts treated with CASIN (representative pictures). Scale bar, 100 μ m

(B) Percentage of organoid growth after third passage culture of organoids formed from young and aged intestinal crypts treated with and without CASIN

(C) Number of lobes per organoid after third passage culture of organoids formed from young and aged intestinal crypts treated with and without CASIN

(D) Organoids from Lgr5 GFP sorted cells from young and aged mouse intestinal crypts with and without CASIN treatment.

(E) Percentage of colonies formed from young and aged Lgr5 GFP+ cells treated with CASIN 5 to 6 days after initial plating. n = 3 to 5 mice/experimental group. *p < 0.05, **p < 0.01, ***p < 0.001. Error bars represent standard deviation (SD).

established radiation stress recovery assay (recovery on day 5 after 10 + 10Gy irradiation on two consecutive days (Figure 4D)) to investigate the extent to which suppression of Cdc42 activity *in vivo* rescues aging-associated regenerative defects of ISCs. In this assay, aged crypts show a reduced regenerative response compared to crypts in young animals (Nalapareddy et al., 2017) (Figures 4E–4G). CASIN-treated aged mice presented with an increase in crypt depth and frequency of crypt fission consistent with an enhanced regenerative response when compared to vehicle-treated aged mice (Figures 4E–4G). Pharmacological suppression of Cdc42 activity *in vivo* appears therefore to be effective in enhancing ISC-driven regeneration upon radiation induced stress in aged crypts.

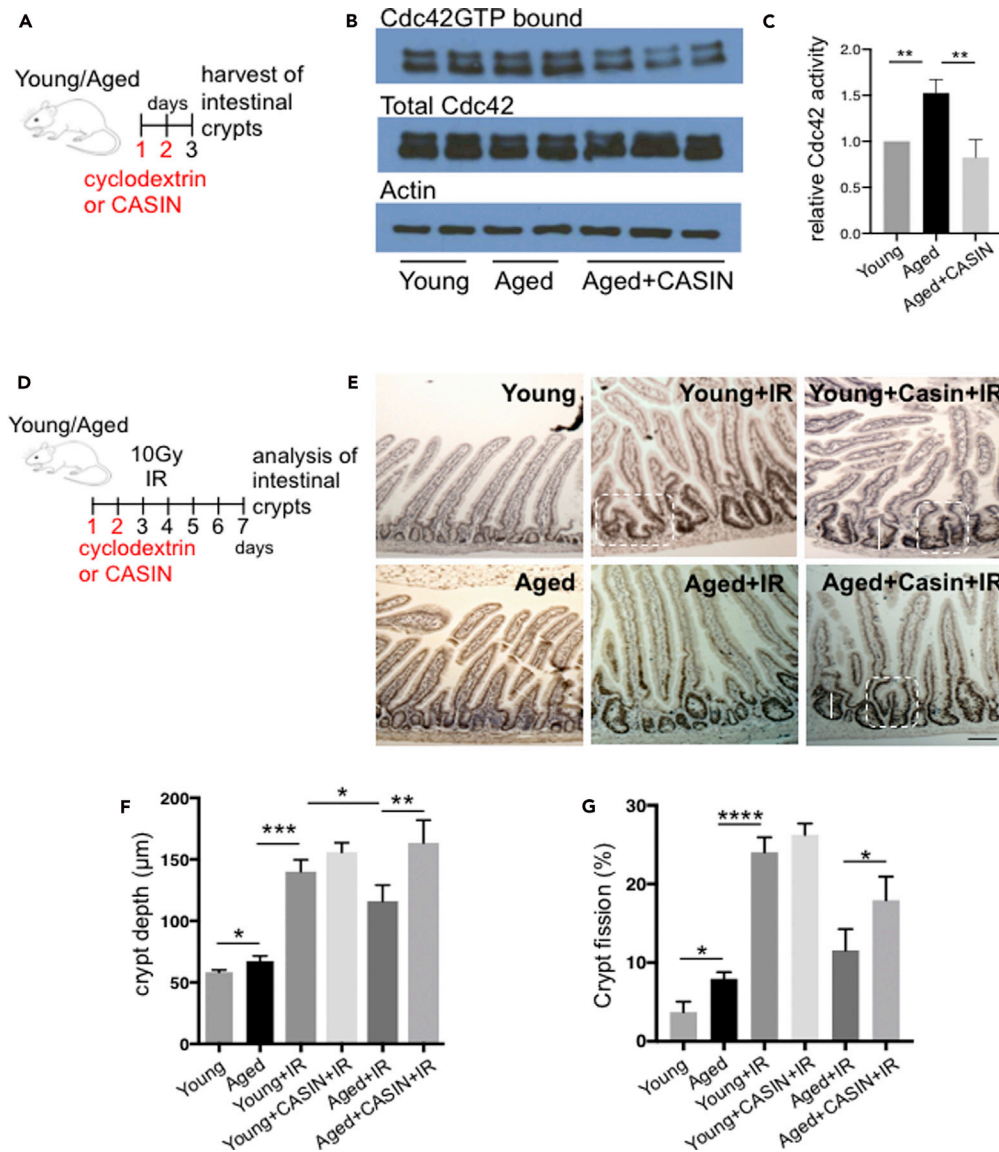


Figure 4. Modulation of Cdc42 activity in crypts *in vivo* enhances the regeneration of aged crypts upon stress

(A) Experimental setup

(B) Western blot of Cdc42 pull-down experiment to quantify the relative amount of Cdc42 GTP, Cdc42, and β -actin protein in crypts from young and aged animals and aged animals treated with CASIN

(C) Relative level of Cdc42 GTP normalized to total Cdc42 and β -actin in crypts from young and aged animals and aged animals treated with CASIN.

(D) Experimental setup for 10 + 10Gy irradiation experiment of young and aged animals treated with vehicle or CASIN to analyze regeneration of crypts

(E) Ki67 staining in young and aged crypts with or without radiation (control) and with CASIN or without CASIN (vehicle alone) treatment (representative pictures)

(F) Crypt depth in the proximal part of mouse small intestine 5 days after 10 + 10-Gy radiation.

(G) Percentage of crypt fission in young and aged crypts 5 days after 10 + 10-Gy radiation. (A to G): n = 3 to 5 mice/ experimental group. *p < 0.05, **p < 0.01, ***p < 0.001. Error bars represent standard deviation (SD).

DISCUSSION

Increased Cdc42 activity is seen in aged intestinal crypts, especially in ISCs and likely also TA cells of the crypts. In ISCs, a reduced expression level of *Ascl2* associated with elevated Cdc42 activity suggests a critical role for the level of expression of *Ascl2* for proper ISC function (Nalapareddy et al., 2017; van der Flier

et al., 2009). Changes in Cdc42 activity appear to be downstream of canonical Wnt signaling, as treatment of organoids derived from crypts of Cdc42GAP knockout mice with a canonical Wnt ligand (Wnt3a) could not rescue the organoid formation ability. In HSCs, being apolar for the distribution of H4K16ac is a direct consequence of an elevated level of Cdc42 activity (Florian et al., 2012, 2018; Grigoryan et al., 2018), and we report here that also aged ISCs show an apolar distribution of H4K16ac. An apolar distribution of H4K16ac indicates epigenetic changes upon aging of ISCs (Grigoryan et al., 2018). Apolar distribution of H4K16ac might thus further serve as a shared hallmark of aged stem cells.

Inhibition of Cdc42 activity in aged ISCs enhanced the ability to form organoids, suggesting that reducing Cdc42 activity in aged ISCs is sufficient to restore a more youthful phenotype. This coins our observation that pharmacological inhibition of Cdc42 activity attenuates aging-related impaired stress-induced crypt regeneration and in part a consequence of a change in ISC function *in vivo* upon CASIN treatment. While overall our data strongly imply a critical role of elevated activity of Cdc42 in ISCs for aging-related changes in crypt function, it remains still a possibility that in addition to the action in ISCs, elevated activity of Cdc42 in non-ISCs like TA cells (Figure 1) might act indirectly on ISCs and crypt function. For example, it was recently shown that the Wnt inhibitor Notum regulates Wnt signaling and thus ISC function indirectly through Paneth cells (Pentimikko et al., 2019), so additional experiments will need to reveal the magnitude of the extent of stem cell extrinsic contribution of elevated Cdc42 activity to aging of ISCs. In summary, we provide evidence that the decline of the ISC-driven regeneration potential of aged crypts can be ameliorated via pharmacological interventions. Alteration of mechanisms other than canonical Wnt signaling in intestinal compartment could also help to revamp the aging-associated decline in ISC function.

Limitations of the study

Our data are consistent with a critical role of elevated Cdc42 activity in aged ISCs for a reduced regenerative capacity of aged ISCs (Figures 4B and 4C). To test Cdc42 activity directly in ISCs is very difficult because we cannot reliably determine the expected 1.5 to 2-fold difference simply by IF staining (see Figures 1F, 1G, and 4A–4C) and cannot really perform pull-down assays on ISCs due to the requirement of large number of cells for the pull-down assay. It is thus still a possibility that indirect effects outside these ISCs intrinsic mechanisms might, in addition to elevated Cdc42 activity in ISCs, contribute to aging-associated phenotypes of ISCs. In addition, we do not fully understand the biology of Cdc42 and its changes in activity in young cells, including young ISCs and crypts *in vivo*. The fact that CASIN had no effect on the function of young ISCs therefore remains to be further investigated.

Resource availability

Lead contact

Further information and requests for resources should be directed to and will be fulfilled by the lead contact, Prof. Hartmut Geiger, Hartmut.geiger@uni-ulm.de

Material availability

This study did not generate nor use any new or unique reagents.

Data and code availability

This study did not generate any new huge data sets or used any new codes.

METHODS

All methods can be found in the accompanying [transparent methods supplemental file](#).

SUPPLEMENTAL INFORMATION

Supplemental information can be found online at <https://doi.org/10.1016/j.isci.2021.102362>.

ACKNOWLEDGMENTS

Work in the laboratory was supported by grants from the NIH (R01DK104814, R01 AG063967, P30 DK078392 and AG040118). We thank Zheng Zhang from the Yi Zheng laboratory for providing Cdc42 $-/-$ crypts. We also thank the flow core and the Comprehensive Mouse and Cancer Core at CCHMC. We also thank Confocal Imaging Core at CCHMC.

AUTHOR CONTRIBUTIONS

K.N. performed all the experiments. A.H helped with independent quantification IHC and IF picture. L.S. performed in situ hybridizations. Y.Z. provided CASIN and Cdc42GAP knockout mice and supported data interpretation. H.G. conceived the project. K.N. and H.G. designed the experiments and wrote the manuscript.

DECLARATION OF INTERESTS

H.G and Y.Z are inventors on patent US20150297563A1, Rejuvenation of precursor cells, which comprises, among others, methods of rejuvenating intestinal tissue via inhibition of GTPases.

Received: April 7, 2020

Revised: February 8, 2021

Accepted: March 23, 2021

Published: April 23, 2021

REFERENCES

- Barker, N., van de Wetering, M., and Clevers, H. (2008). The intestinal stem cell. *Genes Dev.* 22, 1856–1864.
- Barker, N., van Es, J.H., Kuipers, J., Kujala, P., van den Born, M., Cozijnsen, M., Haegebarth, A., Koring, J., Begthel, H., Peters, P.J., et al. (2007). Identification of stem cells in small intestine and colon by marker gene *Lgr5*. *Nature* 449, 1003–1007.
- Florian, M.C., Dorr, K., Niebel, A., Daria, D., Schrezenmeier, H., Rojewski, M., Filippi, M.D., Hasenberg, A., Gunzer, M., Scharfetter-Kochanek, K., et al. (2012). Cdc42 activity regulates hematopoietic stem cell aging and rejuvenation. *Cell Stem Cell* 10, 520–530.
- Florian, M.C., Klose, M., Sacma, M., Jablanovic, J., Knudson, L., Nattamai, K.J., Marka, G., Vollmer, A., Soller, K., Sakk, V., et al. (2018). Aging alters the epigenetic asymmetry of HSC division. *PLoS Biol.* 16, e2003389.
- Geiger, H., de Haan, G., and Florian, M.C. (2013). The ageing haematopoietic stem cell compartment. *Nat. Rev. Immunol.* 13, 376–389.
- Grigoryan, A., Guidi, N., Senger, K., Liehr, T., Soller, K., Marka, G., Vollmer, A., Markaki, Y., Leonhardt, H., Buske, C., et al. (2018). LaminA/C regulates epigenetic and chromatin architecture changes upon aging of hematopoietic stem cells. *Genome Biol.* 19, 189.
- Liu, W., Du, W., Shang, X., Wang, L., Evelyn, C., Florian, M.C., Ryan, R., Rayes, A., Zhao, X., Setchell, K., et al. (2019). Rational identification of a Cdc42 inhibitor presents a new regimen for long-term hematopoietic stem cell mobilization. *Leukemia* 33, 749–761.
- Nalapareddy, K., Nattamai, K.J., Kumar, R.S., Karns, R., Wikenheiser-Brokamp, K.A., Sampson, L.L., Mahe, M.M., Sundaram, N., Yacyshyn, M.B., Yacyshyn, B., et al. (2017). Canonical Wnt signaling ameliorates aging of intestinal stem cells. *Cell Rep.* 18, 2608–2621.
- Pentimikko, N., Iqbal, S., Mana, M., Andersson, S., Cognetta, A.B., 3rd, Suci, R.M., Roper, J., Luopajarvi, K., Markelin, E., Gopalakrishnan, S., et al. (2019). Notum produced by Paneth cells attenuates regeneration of aged intestinal epithelium. *Nature* 571, 398–402.
- Rando, T.A. (2006). Stem cells, ageing and the quest for immortality. *Nature* 441, 1080–1086.
- Rossi, D.J., Jamieson, C.H., and Weissman, I.L. (2008). Stems cells and the pathways to aging and cancer. *Cell* 132, 681–696.
- Sato, T., van Es, J.H., Snippert, H.J., Stange, D.E., Vries, R.G., van den Born, M., Barker, N., Shroyer, N.F., van de Wetering, M., and Clevers, H. (2011). Paneth cells constitute the niche for *Lgr5* stem cells in intestinal crypts. *Nature* 469, 415–418.
- van der Flier, L.G., van Gijn, M.E., Hatzis, P., Kujala, P., Haegebarth, A., Stange, D.E., Begthel, H., van den Born, M., Guryev, V., Oving, I., et al. (2009). Transcription factor achaete scute-like 2 controls intestinal stem cell fate. *Cell* 136, 903–912.
- Wang, L., Yang, L., Debidda, M., Witte, D., and Zheng, Y. (2007). Cdc42 GTPase-activating protein deficiency promotes genomic instability and premature aging-like phenotypes. *Proc. Natl. Acad. Sci. U S A* 104, 1248–1253.
- Wang, L., Yang, L., Filippi, M.D., Williams, D.A., and Zheng, Y. (2006). Genetic deletion of Cdc42GAP reveals a role of Cdc42 in erythropoiesis and hematopoietic stem/progenitor cell survival, adhesion, and engraftment. *Blood* 107, 98–105.

iScience, Volume 24

Supplemental information

**Suppression of elevated Cdc42 activity
promotes the regenerative potential
of aged intestinal stem cells**

**Kodandaramireddy Nalapareddy, Aishlin Hassan, Leesa L. Sampson, Yi
Zheng, and Hartmut Geiger**

Supplemental information

Transparent Methods

Mice

Young (2-3 months) C57BL/6 mice were purchased from Charles River, aged mice (18 to 22 months) obtained from the NIA colony. *Cdc42GAP*^{-/-} mice (Wang et al., 2007; Wang et al., 2006) were provided by in-house breeding. *Lgr5*^{eGFP^{Cre}ER(T2)} mice (Barker et al., 2007) were purchased from Jackson Laboratories. All animals were housed at CCHMC under specific pathogen-free conditions. All animal experiments were approved by the Animal Care and Use Committee of Cincinnati Children's Hospital Medical Center.

Immunofluorescence staining

Analyses were performed on the proximal part of the small intestine. Tissues were fixed overnight in 4% paraformaldehyde (PFA) at 4 °C and washed three times in PBS. Fixed tissues were dehydrated and embedded in paraffin. Immunofluorescence analyses were performed on 6µm thick paraffin sections. Sections were deparaffinized, rehydrated and permeabilized in 10mM sodium citrate buffer. Sorted cells or cells grown on cover slips were fixed immediately with 4% PFA at room temperature, washed twice with 1X PBS and stored at 4°C. Sorted cells were cytopspin on to slides (500rpm for 2 minutes), fixed again with 4%PFA, washed twice with 1X PBS, permeabilized with 0.2% Triton X and washed twice with 1XPBS. Primary antibodies were incubated overnight at 4°C: anti-Cdc42 (1/100 dilution in PBS), anti-Cdc42GTP (1/50 or 1/150 dilution in PBS, 0.5%BSA, 0.5% Tween 20), anti-Ki67 (1/100 dilution in PBS), anti-lysozyme (1/100 dilution in PBS), anti-MMP7 (1/100 dilution in PBS), anti-phospho Histone 3 antibody (cell signaling technology, 1:100 in PBS) and anti-GFP antibody (Santa Cruz 1:100 in PBS) followed by washing with PBS and incubation with secondary antibodies anti-mouse-FITC (Jackson laboratories, 1:200 in PBS) or anti-rabbit-Cy3 (Jackson Laboratories, 1:200 in PBS) for 1 h at

room temperature. For cryo-embedding, fixed tissues were incubated overnight in 30% sucrose in PBS at 4 °C and then embedded in Optimal Cutting Temperature compound (OCT; Sakura); sections were cut at 7µm thickness. Tissues were permeabilized in 0.3% TritonX for 10 mins or permeabilized in 10mM sodium citrate buffer at boiling temperature for 2 mins, washed with PBS and stained for GFP and Cdc42GTP, following the protocol above.

Cryo sections were used for Lgr5 RNAscope analysis and followed manufacturer's instructions for FISH (Fluorescent In situ hybridization). In short, 7 to 9µ cryo sections were thawed to room temperature and washed with 1X PBS. Samples were fixed in 3.7% Formaldehyde in 1X PBS for 10 mins, followed by 2 washes with 1x PBS. Samples were incubated with Proteinase K (Ambion, 10µg/ml in 1xPBS) for 10 to 20 minutes followed by 2 washes with 1X PBS and a 5 minutes wash with 2xSSC with 10% deionized formamide (Wash buffer). 12.5µM mouse Lgr5 probe (Stellaris® FISH Probes, Mouse Lgr5 with CAL Fluor® Red 590, BioResearch analysis) is diluted (1/50 dilution) with hybridization buffer from the manufacturer and incubated in humid chamber at 37°C overnight in dark followed by washing with wash buffer with 5ng/ml DAPI for 10 mins. Washed again with wash buffer for 10 mins. Finally washed for 5 mins with TBS-T for 5 mins and mounted the slides with fluorescent mounting medium and proceeded to confocal microscopy.

Crypt and ISCs isolation and organoid assays and gene expression analysis

Mouse small Intestine was dissected and washed in cold PBS. Villi were removed by scraping the tissue with glass slides. Intestinal pieces were transferred to 5mM EDTA in PBS (pH 8), followed by three times 1min shaking by hand with a 10 min incubation at 4°C. Intestinal pieces were removed, centrifuged at 149g for 5 min and the pellet was resuspended in PBS followed by centrifugation at 84g for 2 min. Isolated crypts were immediately used for organoid cultures or frozen at -80°C for further experiments. Isolated crypt epithelial cells from the proximal part of the

small intestine were used for gene expression analysis by quantitative RT-PCR. RNA was isolated using the QIAGEN RNeasy minikit. Fifty nanograms of RNA were used per well in a single-step Taqman assay. Normalization was done using β Actin. FAM-Labeled Real-Time PCR Primers for mouse (ABI) were used.

For the ISCs colony formation assay, isolated crypts were treated with 30 mL of 4% TrypLE (Invitrogen) for 30–40 min at 37°C, followed by centrifugation at 149g for 5 min. The pellet was resuspended in 15 mL DMEM and centrifuged again at 84g. The supernatant was discarded and Lgr5eGFP^{hi} cells sorted by FACS. 500 cells, plated on matrigel – ISC medium (1:29 ratio) in a 96 well plate with ISC medium (Nalapareddy et al., 2017) containing 500ng/ml of R-spondin, Wnt3a 10ng/ml. For first 24 to 48 hrs ISC medium with Thiazovivin 2 μ M (Sigma Aldrich), Jag1 1 μ M (Anaspec), Y-27632 dihydrochloride 1 μ M (upgraded ISC medium) was used to culture isolated ISC. After 48 hrs, regular ISC medium with 100ng/ml Wnt3a and 500ng/ml more R-spondin was used for further culture. For CASIN treatment, crypts or ISCs were incubated for 16 hours with 0.5 μ M CASIN (Liu et al., 2019) dissolved in Cyclodextrin (vehicle) or vehicle alone in ISC medium. The medium was changed every alternative day thereafter. Colonies for ISC cultures were counted on 5th or 6th day after the initial plating.

For crypt organoid cultures, our previously published protocol was used (Nalapareddy and Geiger, 2020; Nalapareddy et al., 2017). In short, 500 isolated crypts were plated in ISC medium in matrigel and cultured at 37°C in ISC medium with and without CASIN (0.5 μ M) or vehicle alone for 16 hours and medium was changed every alternative day thereafter. For Wnt3a experiments, 100ng/ml of mouse recombinant Wnt3a (Peprotech) was added to the medium. Organoids were quantified after 3rd or 4th passage for young and aged. Cdc42GAP^{-/-} organoids were quantified 6 days after initial plating as they barely form organoids in after 1st passage.

Cdc42-GTP pull down assay

Whole cell extracts of mouse proximal intestinal crypt epithelial cells were obtained in RIPA lysis

buffer. Cdc42 activity can be determined by a pulldown-assay (Wang et al., 2006) using (Rac/Cdc42 Assay reagent, PAK-1, PBD conjugate, Millipore) according to the protocol of the manufacturer. Protein was subjected to standard SDS-PAGE, blotted onto a PVDF membrane and detected using antibodies against Cdc42 (1:1000 dilution, abcam), Actin (1:1000 dilution, Sigma). The intensity of Cdc42-GTP was normalized to intensity of total Cdc42 (ratio of the densitometric score of the Cdc42-GTP form and the total Cdc42 form).

Pull down for NIH3T3 cells were performed on serum starved NIH3T3 cells with 0.5% FBS for 48 hours and stimulated them with regular 5% FBS and samples were harvested after 16 hours and whole cell extracts are isolated as described above. Cells plated on cover slips were used for Cdc42GTP IF experiments at the same point.

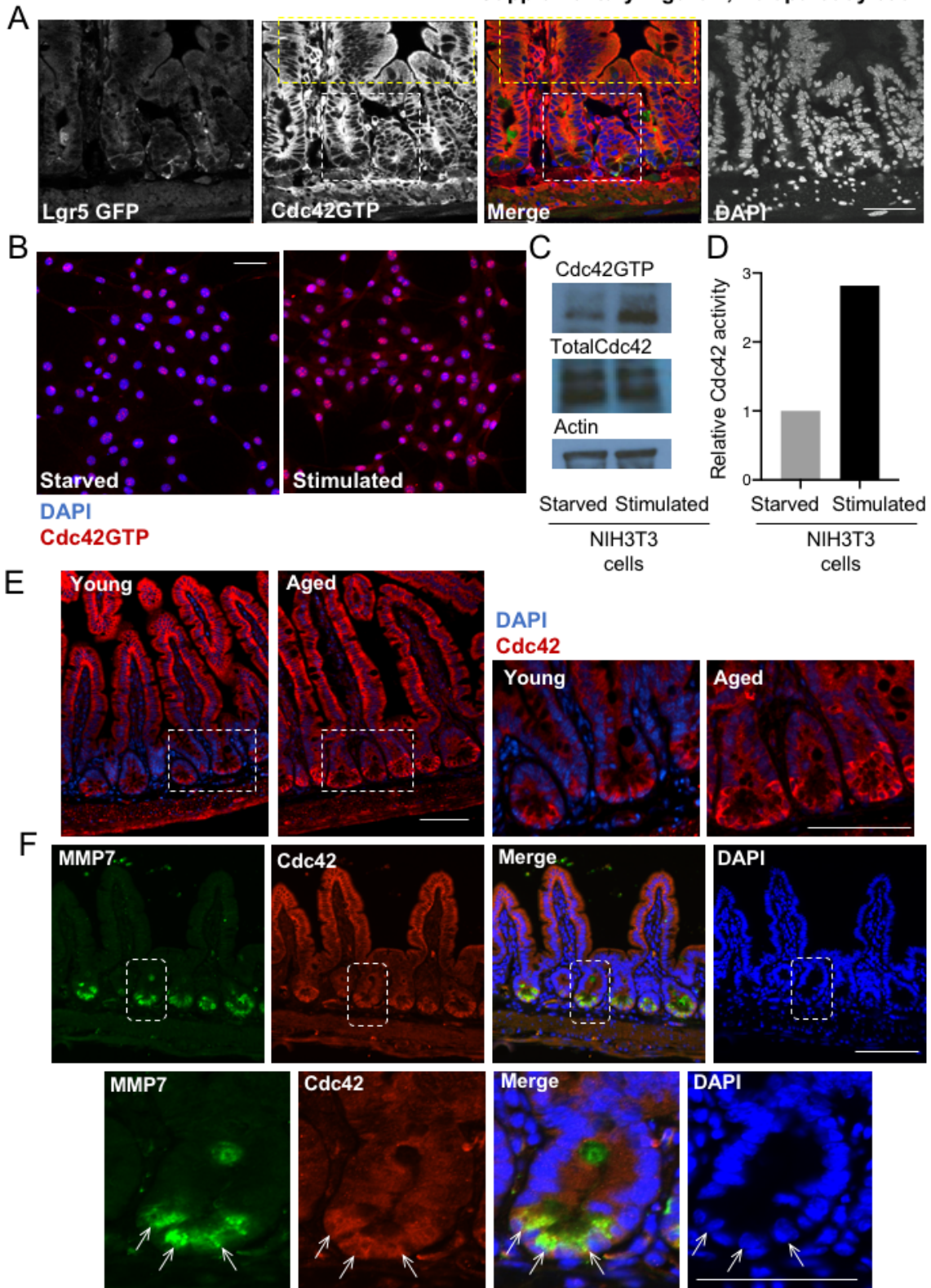
***In vivo* CASIN treatment and irradiation recovery**

Mice received intraperitoneal injections of CASIN (50mg/kg body weight) or Cyclodextrin (vehicle) on day one and day two. On day three and day four, mice were irradiated with 10 Gy each day (I-68A cesium 137 irradiator, JL Shepherd & Associates). Tissue was harvested 5 days after the first irradiation (Nalapareddy et al., 2017).

Statistical Analyses To calculate statistical significance, either a Student's t test or a Wilcoxon/Mann-Whitney test was used. Error bars indicate SD. GraphPad Prism or Microsoft Excel was used for statistical analysis.

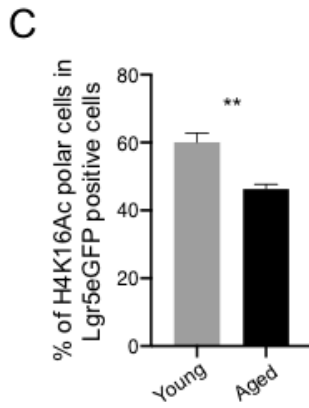
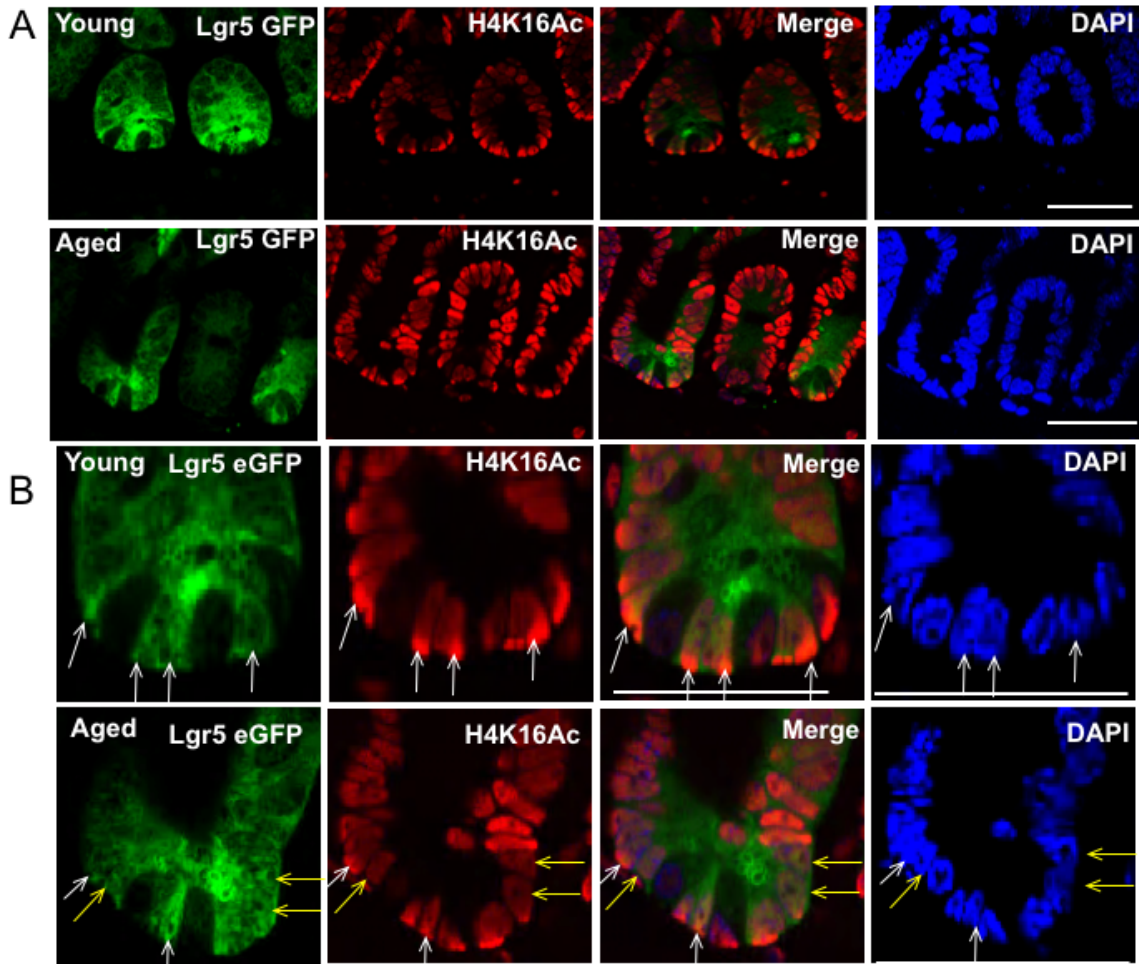
SUPPLEMENTARY FIGURES AND FIGURE LEGENDS

Supplementary Figure 1, Nalapareddy et al



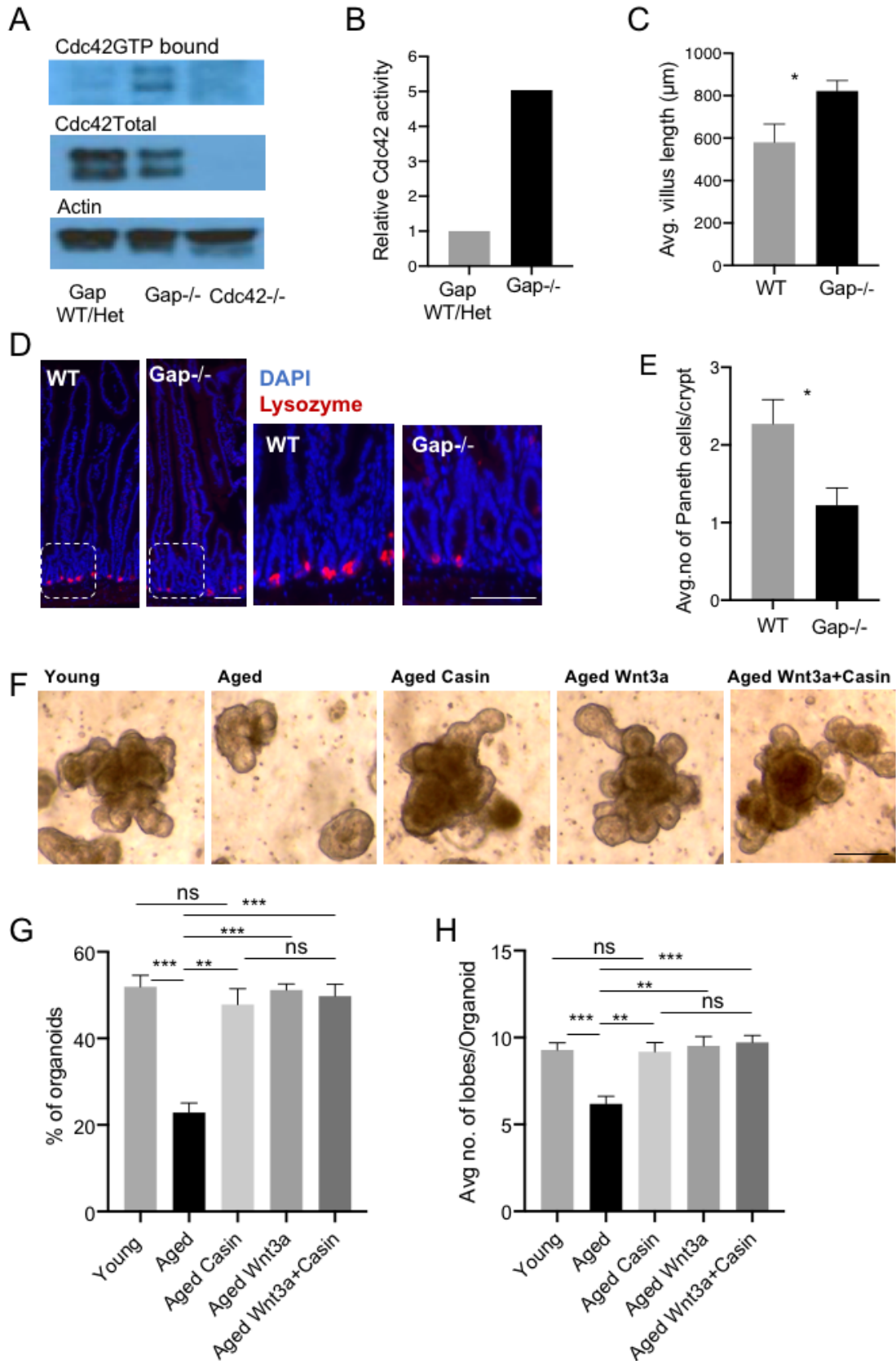
Supplementary Figure 1. Cdc42 GTP staining, Cdc42GTP pull down and Cdc42 staining, related to Figure 1(A). Representative black and white pictures of Cdc42 GTP showing Cdc42GTP positive crypts (white box, strong staining in the cytoplasm) while Cdc42GTP remains low in villi (yellow box, Cdc42GTP staining remains low around the nucleus of cells. Scale bar 50 μ m (Young mouse intestine). (B) Representative pictures of immunofluorescence staining of NIH3T3 cells with serum starvation and 16 hours after serum stimulation. Scale bar 50 μ m. (C) Western blot of Cdc42GTP pull down experiment to quantify the relative amount of Cdc42 GTP, Cdc42 and β -actin protein in NIH3T3 cells with indicated treatments. (D) Relative levels of Cdc42 GTP normalized to total Cdc42 in NIH3T3 cells with serum starvation and 16hours after serum stimulation. (E) Representative pictures of Cdc42 staining in young and aged intestinal crypts. Scale bar 100 μ m, zoomed in pictures for dotted boxes respectively, Scale bar 100 μ m. (F) Representative pictures of Cdc42 (Red), MMP7 (Green) and Dapi (Blue) co-staining in young mouse intestinal crypts, Scale bar 100 μ m, zoom in pictures for dotted boxes respectively Scale bar 50 μ m. n=3 to 5 mice/Experimental group. *p < 0.05, **p < 0.01, ***p < 0.001. Error bars represent SD

Supplementary Figure 2, Nalapareddy et al



Supplementary Figure 2. H4K16 acetylation, related to Figure 1 (A) Immunofluorescence staining of H4K16Ac (red), Lgr5eGFP (green) and DAPI (blue) in crypts of young and aged mice. (representative pictures, scale bar 50 μ m). (B) Zoomed in Immunofluorescence staining of H4K16Ac (red), Lgr5eGFP (green) and DAPI (blue) in crypts of young and aged mice. (representative pictures, scale bar 50 μ m). White arrows indicate cells with a polar distribution of H4K16Ac, yellow arrows indicate cells with an apolar distribution of H4K16ac. (C) Frequency of ISCs (Lgr5eGFP positive cells) polar for the distribution of H4K16Ac in young and aged murine intestinal crypts. (A to C): n=3 to 5 mice/experimental group. *p < 0.05, **p < 0.01, ***p < 0.001. Error bars represent SD.

Supplementary Figure 3, Nalapareddy et al



Supplementary Figure 3. Analysis of Cdc42 Gap^{-/-} mice, related to Figure 2 (A) Western blot of Cdc42 pull down experiment to quantify the relative amount of Cdc42 GTP, Cdc42 and β -actin protein in the crypts of WT litter mate controls, Gap^{-/-} mice and Cdc42^{-/-} Villin Cre mice (From Yi Zhang's lab). (B) Relative levels of Cdc42 GTP normalized to total Cdc42 (n=3 per group, pooled, n=1 for Cdc42^{-/-} mouse) in the indicated genotypes. (C) Histogram showing Villus length in the proximal part of WT litter mate controls and Gap^{-/-} mice. (D) Representative immunofluorescence staining of Lysozyme (Red) and DAPI (Blue) in the indicated genotypes. (E) Histogram showing average number of Paneth cells (Lysozyme positive cells) per crypt in the indicated genotypes. (F) Organoids formed from young and aged intestinal crypts treated with CASIN or Wnt3a or Wnt3a+Casin (representative pictures) 5 days after 3rd passage of organoid culture. Scale bar 100 μ m (G) Percentage of organoid growth 5 days after 3rd passage of the culture of organoids formed from young and aged intestinal crypts with the indicate treatments (H) Number of lobes per organoid 5 days after 3rd passage of the culture of organoids formed from young and aged intestinal crypts with indicated treatments. n=3 mice/experimental group. *p < 0.05, **p < 0.01, ***p < 0.001. Error bars represent SD.

Barker, N., van Es, J.H., Kuipers, J., Kujala, P., van den Born, M., Cozijnsen, M., Haegebarth, A., Korving, J., Begthel, H., Peters, P.J., *et al.* (2007). Identification of stem cells in small intestine and colon by marker gene *Lgr5*. *Nature* *449*, 1003-1007.

Liu, W., Du, W., Shang, X., Wang, L., Evelyn, C., Florian, M.C., M, A.R., Rayes, A., Zhao, X., Setchell, K., *et al.* (2019). Rational identification of a *Cdc42* inhibitor presents a new regimen for long-term hematopoietic stem cell mobilization. *Leukemia* *33*, 749-761.

Nalapareddy, K., and Geiger, H. (2020). Analysis of Aged Dysfunctional Intestinal Stem Cells. *Methods Mol Biol* *2171*, 41-52.

Nalapareddy, K., Nattamai, K.J., Kumar, R.S., Karns, R., Wikenheiser-Brokamp, K.A., Sampson, L.L., Mahe, M.M., Sundaram, N., Yacyshyn, M.B., Yacyshyn, B., *et al.* (2017). Canonical Wnt Signaling Ameliorates Aging of Intestinal Stem Cells. *Cell reports* *18*, 2608-2621.

Wang, L., Yang, L., Debidda, M., Witte, D., and Zheng, Y. (2007). *Cdc42* GTPase-activating protein deficiency promotes genomic instability and premature aging-like phenotypes. *Proceedings of the National Academy of Sciences of the United States of America* *104*, 1248-1253.

Wang, L., Yang, L., Filippi, M.D., Williams, D.A., and Zheng, Y. (2006). Genetic deletion of *Cdc42GAP* reveals a role of *Cdc42* in erythropoiesis and hematopoietic stem/progenitor cell survival, adhesion, and engraftment. *Blood* *107*, 98-105.